Int. J. Nanoscience, 11, 2012, 1-7

The Fatigue and Fracture Behaviour of Micron-Rubber and Nano-Silica Modified Epoxy Polymer

C.M. Manjunatha*, N. Jagannathan

Structural Technologies Division, CSIR-National Aerospace Laboratories, Bangalore-560017, India,

A.C. Taylor, A.J. Kinloch

Department of Mechanical Engineering, Imperial College London, South Kensington Campus, London, SW7 2AZ, UK

ABSTRACT

A thermosetting epoxy polymer was modified by incorporating 9 wt. % of CTBN rubber micro particles. The neat (ie., unmodified) and the rubber-modified epoxy resins were poured into release-coated steel moulds and cured to prepare bulk epoxy sheets from which the standard fatigue test specimens were machined. Stress-controlled, constant-amplitude fatigue tests were conducted using dog-bone shaped test specimens, at a stress ratio, $R = \sigma_{min}/\sigma_{max} = 0.1$ with sinusoidal waveform at 3 Hz. The fatigue crack growth rate tests were conducted using compact tension specimens at stress ratio, R=0.1. The fatigue life was higher by about three to four times and fatigue crack growth rates were lower by over an order of magnitude in the rubber-modified epoxy polymer when compared to that of neat epoxy polymer. The energy dissipating mechanisms of rubber particle cavitation and plastic deformation were observed to be operative, resulting in this improved fatigue behavior. The fatigue crack initiation and propagation lives estimated from the experimental data suggested that the combined effects of (i) delayed crack initiation, (ii) retarded crack growth rate and, (iii) improved fracture toughness resulting in higher critical crack length for fatigue fracture, all contribute to the enhanced fatigue life of the rubber-modified epoxy polymer.

* Corresponding author: Tel.: +91 80 2508 6310; Fax: +91 80 2508 6301

E-mail address: manjucm@nal.res.in (CM Manjunatha)

Key words: Epoxy polymer, rubber particle, fatigue, crack growth

1. INTRODUCTION

Due to their high specific strength and stiffness, fibre reinforced plastic (FRP) composites are widely used in various structural applications and they invariably experience cyclic-fatigue loads in service. These FRP composites generally consist of continuous fibres of glass, or carbon, reinforced in a thermosetting epoxy polymer. The epoxy polymer used is amorphous and a highly cross-linked material. It is relatively brittle and has a poor resistance to crack initiation and growth. These adverse properties of the epoxy matrix affect the overall fatigue and fracture performance of the FRP composites.

One of the ways to enhance the fatigue and fracture properties of FRP composites is to improve the corresponding properties of the epoxy matrix by incorporating second-phase modifiers in the resin. Various types of micro- and nano-sized particles, such as rubber and silica, have been employed [1-12]. The well-dispersed rubber micro-particles, in the range of 5 to 20 vol.%, in the epoxy has been shown to significantly improve the fracture toughness of bulk epoxy polymers [1,2,4]. Further, FRP composites based upon rubber-particle reinforced matrices, have also shown a significant improvement in their values of interlaminar fracture toughness [6,7]. Fatigue crack growth rates have been observed to reduce by addition of rubber particles in the epoxy polymer [4,5,8]. The main aim of this investigation was to study further in detail, the effect of addition of CTBN rubber particles on the fatigue behaviour of epoxy polymer. An attempt is made to analyze the contribution of crack initiation and crack propagation life on the enhancement of total fatigue life of a rubber modified thermosetting epoxy polymer.

2. EXPERIMENTAL

2.1 Materials

The materials were based upon a single-component hot-cured epoxy formulation. The epoxy resin was a standard diglycidyl ether of bis-phenol A (DGEBA) with an

epoxide equivalent weight (EEW) of 185 g/mol, 'LY556' supplied by Huntsman, Duxford UK. The reactive liquid rubber, which gives rises to the micrometer-sized spherical rubber particles upon curing of the formulation, was a carboxyl-terminated butadiene-acrylonitrile (CTBN) rubber. It was supplied by Emerald Materials, Akron, USA, and was 'Hycar CTBN 1300 x 8' with a number-average molecular weight of 3550 g/mol and an acrylonitrile content of 18 wt.%. This was pre-reacted with the DGEBA resin to give a 40 wt.% CTBN-epoxy adduct: 'Albipox 1000' (EEW =330 g/mol) from Nanoresins, Geesthacht, Germany. The curing agent was an accelerated methylhexahydrophthalic acid anhydride, 'Albidur HE 600' (AEW =170 g/mol) also supplied by Nanoresins.

2.2 Processing

The required quantity of the neat DGEBA epoxy resin was weighed and degassed at 50^0C. The calculated quantity of CTBN-epoxy adduct, to give the required level of 9 wt.% added CTBN rubber in the final resin mixture was also weighed and degassed. They were then mixed together and the value of the EEW of the blend was measured via titration. The stoichiometric amount of curing agent was added to the mixture. The entire resin mixture was then stirred and degassed once again at 50 ^{0}C and -1 atm. for about an hour. The resins (neat and rubber-modified) were poured into a release-coated steel moulds. The filled moulds were then placed in a circulating air oven and the temperature was ramped to 100^0C at 1^0C/min, cured for 2 hours, again ramped to 150^0C at 1^0C/min and post-cured for 10 hours. The resulting unmodified and rubber-modified bulk epoxy sheets were about 200 mm x 200 mm x 5 mm in size.

2.3 Microstructure

The atomic force microscope (AFM) was used to observe the bulk epoxy polymer microstructure. A smooth surface was first prepared by cutting samples on a microtome at room temperature. The scans were performed in tapping mode using silicon probes. The AFM phase image of the rubber-modified bulk epoxy polymer is shown in Fig. 1. It was observed that the rubber particles were evenly distributed

and had an average size of about 0.5 to 1 μm. The average inter particle distance measured was about 2.45 μm.

2.4 Tensile Properties

The tensile properties of the bulk epoxies were determined according to ASTM D638 test standard [13] specifications. The dog bone shaped tensile test specimens, as shown schematically in Fig. 2(a), were cut and prepared from the bulk epoxy sheets. Tensile tests were performed in a 100 kN computer controlled screw-driven test machine with a constant crosshead speed of 1 mm/min. Extensometer with a 25 mm gage length was used for strain measurements. Five numbers of tests were conducted for each material and the average tensile properties were determined. The typical stress-strain curves determined from the tensile testing of both neat and rubber-modified epoxy polymers are shown in Fig. 3 and the average tensile properties determined are shown in Table 1. Due to soft rubber particles, as observed in earlier investigation [14], the ultimate tensile strength and tensile modulus of the rubber modified epoxy polymer decrease by about 11 % and 19 % respectively.

2.5 Fatigue Testing

Two types of fatigue tests were conducted on both neat and rubber modified epoxy polymers. Constant amplitude fatigue tests were conducted to determine stress-life (S-N) curves and fatigue crack growth tests (da/dN Vs ΔK) were performed to determine crack speeds. Stress-controlled, constant amplitude fatigue tests were performed using dog-bone shaped test specimens shown schematically in Fig. 2 (a). The sharp edges of the test specimens were smoothed with emery paper, before testing, to avoid any stress concentration effects. All the fatigue tests were performed using a 25 kN computer-controlled servo-hydraulic test machine. The following fatigue parameters were employed for the tests: stress ratio, R = 0.1, sinusoidal waveform and frequency, ν = 3 Hz.

Fatigue crack growth tests were performed using 50 mm wide standard compact tension (CT) test specimens shown schematically in Fig. 2 (b). The fatigue

crack growth tests were performed in a computer controlled 50 kN servo-hybdraulic test machine as per ASTM E647 test standard [15] specifications. The specimens were pre-cracked under cyclic loads and then decreasing ΔK test was conducted to obtain crack growth rates in the near-threshold regime. Further, constant load, increasing ΔK test was conducted to obtain growth rates in the Paris' and high ΔK regimes. The crack length was monitored by compliance technique using a crack opening displacement (COD) gage.

The failed fatigue fracture surfaces of the bulk epoxy specimens were examined in scanning electron microscope (SEM). The fracture surfaces were sputter coated with a thin layer of gold, to prevent charging. Conventional secondary electron imaging conditions with an accelerated voltage of 15 kV was employed in SEM.

3. RESULTS AND DISCUSSION

3.1 Stress-life (S-N) behaviour

The constant-amplitude, tension-tension, cyclic-fatigue test results obtained for both neat and rubber modified epoxy polymers at a stress ratio, R=0.1, are shown in Fig. 4. Here the vertical axis represents the maximum cyclic stress applied in the fatigue cycle and the horizontal axis represents the number of cycles to failure, i.e. typical 'S-N' curves. It may be clearly seen that, for a given maximum cyclic stress, the fatigue life of the 9 wt.% rubber-modified epoxy polymer is higher than that of the neat epoxy, by about three to four times, and that this fatigue life enhancement appears over the entire range of the stress level investigated.

The experimental S-N data shown in Fig. 4 was fitted to Basquin's law [28]:

$$\sigma_{max} = \sigma_f^{'} (N_f)^{b} \qquad (1)$$

where $\sigma_f^{'}$ is the fatigue strength coefficient (FSC) and 'b' is the fatigue strength exponent (FSE). The values of the parameters FSC and FSE, determined for both the neat and rubber-modified epoxy polymers, are shown in Table 2. It can be seen that the presence of the rubber increases the value of the FSC by about 35%, whilst that of the FSE was observed to decrease by about 16%. It is of interest to note that

Zhou et al. [16] have also observed very similar trends in the variation of the fatigue properties for an epoxy polymer modified with carbon nanofibres.

Typical appearance of the failed fatigue fracture surface of test specimens, as observed in SEM at low magnifications, is shown in Fig. 5. In general, the fatigue crack was observed to initiated from the specimen surface and propagate inside in the form of a semi-elliptical, i.e. thumbnail, shaped crack. In accordance with general observations in polymers [17], a smooth, mirror-like region was exhibited by this initial fatigue crack growth region (D-shaped region), which was followed by a radially-lined, relatively rough, fast-fracture region as shown in Fig. 5. It may be noted that the crack growth region was clearly identifiable in rubber-modified epoxy (D-shaped region in Fig. 5 (b)) but was difficult in neat epoxy due probably to low fracture toughness resulting in very small critical crack lengths at which fast fracture occurs.

Considering the appearance of observed fracture surfaces of epoxy polymers (Fig. 5), the shape of the fatigue crack which initiated and grew in the test specimen may be idealized as shown schematically in Fig. 6. An empirical equation for the stress intensity factor (SIF), K for a semi-elliptical surface crack in a tensile loaded specimen as shown in Fig. 6, is given by [18]:

$$K = \sigma\sqrt{\frac{\pi a}{Q}}F \qquad 0<a/t<1 \tag{2}$$

Where, σ = applied stress, *a* = crack length and t = thickness. The factors F and Q are expressed as:

$$F = \left[M_1 + M_2\left(\frac{a}{t}\right)^2 + M_3\left(\frac{a}{t}\right)^4 \right] f_\phi g f_w \tag{3}$$

$$Q = 1.0 + 1.464\left(\frac{a}{c}\right)^{1.65} \quad \text{for} \quad \left(\frac{a}{c} \le 1\right) \tag{4}$$

$$M_1 = 1.13 - 0.09\left(\frac{a}{c}\right) \tag{5}$$

$$M_2 = -0.54 + \frac{0.89}{0.2 + \left(\frac{a}{c}\right)} \tag{6}$$

$$M_3 = 0.5 - \left[\frac{1.0}{0.65 + (a/c)}\right] + 14\left(1.0 - \frac{a}{c}\right)^{24} \tag{7}$$

$$g = 1 + \left[0.1 + 0.35\left(\frac{a}{t}\right)^2\right](1 - \sin\phi)^2 \tag{8}$$

$$f_\phi = \left[\left(\frac{a}{c}\right)^2 \cos^2\phi + \sin^2\phi\right]^{0.25} \tag{9}$$

$$f_w = \left[\sec\left(\frac{\pi c}{2b}\sqrt{\frac{a}{t}}\right)\right]^{0.5} \tag{10}$$

Since the critical crack length at which fast fracture occurred (D-shaped region of Fig. 5 (b)) was clearly identifiable in rubber modified epoxy, the fracture toughness of this epoxy polymer was estimated using eqn. (2) to Eqn (10). For specimen fatigue tested at σ_{max} = 37 MPa, the measured crack dimensions from Fig. 5 (b) were a_{cr} = 0.651 mm at $\Phi = 90^0$ (the crack front location normal to surface) and 2c = 1.41 mm. The measured specimen dimensions were, 2b = 9.55 mm and t = 5.08 mm. Using this data, the calculated cyclic fracture toughness of the rubber modified epoxy polymer, was 1.16 MPa√m. Kinloch et al [19] have observed in an earlier investigation that the fracture toughness of the unmodified (i.e. neat) and 9 wt.% rubber modified epoxy polymer was 0.59 MPa√m and 1.11 MPa√m respectively. The fracture toughness estimated from the fatigue test data for rubber modified epoxy thus correlates very well with reported value.

The enhanced fracture toughness in rubber modified epoxy by about a factor of two [19] suggests that, for a given stress level and geometric configurations, the critical crack length at fracture (estimated from eqn. (1)), is improved by about four times. Hence, the D-shaped region in unmodified epoxy is expected to be about 1/4th of the rubber modified epoxy to the order of about 0.15 mm. Neat epoxy thus appears to have very small crack growth life.

3.2 Fatigue crack growth behaviour

The fatigue crack growth rate curves determined for both the neat (i.e, unmodified) and the rubber-modified epoxy polymers, at stress ratio, R =0.1 are shown in Fig. 7. The crack growth rate of rubber modified epoxy polymer was significantly lower, by over an order of magnitude, than that of the unmodified epoxy polymer. The threshold stress intensity factor range, ΔK_{th}, of the neat-epoxy was about 0.23 MPa$\sqrt{m}$. The addition of rubber particles into the epoxy polymer was observed to increase the ΔK_{th}, by about 70%, to about 0.39 MPa$\sqrt{m}$.

The experimental fatigue crack growth rate data shown in Fig. 7 was fitted to Paris' law [20]

$$da/dN = C (\Delta K)^m \quad (11)$$

The Paris' constants, *C* and *m* were determined for both the neat and rubber modified epoxies and are shown in Table 2. Both the Paris constants i.e., coefficient 'C' and exponent 'm' were observed to decrease significantly by the addition of rubber particles in the epoxy polymer. The modified epoxies have been shown to exhibit reduced Paris constants over their respective neat polymers [5,7,8].

The failed fatigue fracture surface of the epoxy polymers was observed in SEM. The neat epoxy polymer exhibited relatively smooth fracture surface and was devoid of any indications of large-scale plastic deformation. However, the rubber-modified epoxy polymer, as shown in Fig. 8 exhibited a relatively rough fracture surface with clear indications of cavitated rubber micro-particles and accompanied plastic deformation of the surrounding epoxy material. Indeed, similar fractographic features have been reported in a rubber-modified epoxy under fatigue loading [5].

The toughening mechanisms in rubber-particle modified epoxy polymers have been investigated extensively [2-8]. The cavitation of rubber particles leads to shear banding of the epoxy matrix and hence, severe plastic deformation of the surrounding material. This energy dissipating mechanism has been shown to reduce the crack propagation rates significantly, up to an order of magnitude [5], resulting in enhanced fatigue life.

3.3 Estimation of Crack Growth Life

The total fatigue life of epoxy polymer may be expressed as:

$$N_t = N_i + N_p \tag{12}$$

Where N_i = crack initiation life and N_p = crack propagation life. By integrating Paris' eqn. (11), the crack growth life, N_p can be obtained:

$$\int_{N_i}^{N_f} dN = \int_{a_i}^{a_f} \frac{da}{C(\Delta K)^m} \tag{13}$$

The crack propagation life, N_p was estimated from eqn (13) as follows: For any given stress level, the fatigue crack was assumed to grow from initial length, a_i = 0.10 mm to final crack length, a_f which was estimated from Eqn. (2). For calculation of a_f, the fracture toughness, K_{IC} of the unmodified (i.e. neat) and 9 wt.% rubber modified epoxy polymer was taken as 0.59 MPa√m and 1.11 MPa√m [19], respectively. Thus integration of eqn (13) between the limits N_i=0; a_i=0.10 and N_f = estimated life; a_f = critical crack length estimated from eqn (2), was carried out for various stress levels. Numerical methods using MATLAB was used to integrate eqn (13).

The crack growth life, N_p thus calculated at various stress levels for both neat and rubber modified epoxy polymers is shown in Table 3. Knowing the crack growth life and the total fatigue life (estimated from eqn. 1), the crack initiation life was estimated from eqn (12) and shown in Table 3. The crack initiation lives determined for both neat and rubber modified epoxy polymers are shown in Fig. 9. It is quite clear from these results that the neat epoxy exhibits almost no crack growth life whereas rubber modified epoxy exhibits about 30 % crack growth life at all the stress levels considered. For any given stress level, the improved fracture toughness leads to an enhanced critical crack length for fast fracture, which associated with the reduced crack growth rate, significantly improves the fatigue life of the rubber particle modified epoxy polymer. In addition, the crack initiation is also delayed in rubber modified epoxy (Fig. 9) which also contribute to enhance the fatigue life.

4. CONCLUSIONS

The following conclusions may be drawn based on the results obtained in the present investigation:

(i). The addition of 9 wt.% rubber micro particles to a thermosetting epoxy polymer enhance the total fatigue life. The fatigue life was observed to increase over the entire range of stress levels investigated, by a factor of three to four times.

(ii). The fatigue crack growth rate of a rubber particle modified epoxy polymer is over an order of magnitude lower than that of neat epoxy polymer. The threshold stress intensity factor range, ΔK_{th}, of the neat-epoxy was increased from 0.23 MPa$\sqrt{m}$ to about 0.39 MPa$\sqrt{m}$ by the addition of rubber particles.

(iii). The energy dissipating mechanisms of rubber particle cavitation and plastic deformation of the surrounding material were observed to be operative and hence improve the fatigue life of rubber modified epoxy polymer.

(iv). The crack initiation and crack propagation lives estimated from fracture mechanics based approach suggests that the fatigue life enhanced in rubber modified epoxy polymer results due to combined effects of (a) delayed crack initiation, (b) reduced crack growth rate and, (c) increased toughness which results in longer critical crack length up to which fatigue crack can grow.

ACKNOWLEDGEMENTS

Authors Dr. CMM and NJ thank Dr. AR Upadhya, Director and Dr. Satish Chandra, Head, STTD, NAL, Bangalore for their support and encouragement during this work. Dr. S. Sprenger, nanoresins, Germany is thanked for providing the resins for this investigations. The authors would like to thank all the technical support staff members of the Dept. of Mech. Engg., Imperial College, London, and Structural

Technologies Division, NAL, Bangalore for their assistance in the experimental studies.

REFERENCES

[1] Kinloch, A.J., Shaw, S.J., Tod, D.A. and Hunston, D.L. (1983). Deformation and Fracture Behavior of a rubber toughened epoxy: Microstructure and Fracture Studies, *Polymer* ,24(10):1341-1354.

[2] Kinloch, A.J. (2003). Toughening Epoxy Adhesives to Meet Today's Challenges, *MRS Bulletin*, 28(6):445-448.

[3] Arias, M.L., Frontini, P.M. and Williams, R.J.J. (2003). Analysis of the Damage Zone Around the Crack tip for Two Rubber-Modified Epoxy Matrices Exhibiting Different Toughenability, *Polymer*, **44(5)**:1537-1546.

[4] Pearson, R.A. and Yee, A. F. (1991). Influence of Particle Size and Particle Size Distribution on Toughening Mechanisms in Rubber Modified Epoxies, *Journal of Materials Science*, **26(14)**:3828-3844.

[5] Azimi, H.R., Pearson, R.A. and Hertzberg, R.W. (1996). Fatigue of Rubber-Modified Epoxies: Effect of Particle Size and Volume Fraction, *Journal of Materials Science*, **31(14)**:3777-3789.

[6] Low,I.M. and Mai, Y.W. (1988). Micromechanisms of Crack Extension in Unmodified and Modified Epoxy Resins, *Composites Science and Technology*, **33(3)**:191-212.

[7] Lowe, A., Kwon, A.H. and Mai, Y.W. (1996). Fatigue and Fracture Behaviour of Novel Rubber Modified Epoxy Resins, *Polymer,* **37(4)**:565-572.

[8] Imanaka, M., Motohashi, S., Nishi, K., Nakamura, Y. and kimoto, M. (2009). Crack-Growth Behaviour of Epoxy Adhesives Modified With Liquid Rubber and Cross-Linked Rubber Particles Under Mode I Loading, *International Journal of Adhesion and Adhesives*, **29(1)**:45-55.

[9] Kinloch, A.J., Masania, K., Taylor, A.C., Sprenger, S. and Egan D. (2008). The Fracture of Glass Fiber Reinforced Epoxy Composites Using Nanoparticle Modified Matrices, *Journal of Materials Science,* **43(3)**:1151-1154.

[10] Higashino, M., Takemura, K. and Fujii, T.J. (1995). Strength and Damage Accumulation of Carbon Fabric Composites with a Cross-Linked NBR Modified Epoxy Under Static and Cyclic Loadings, *Composite Structures,* **32(1-4)**:357-366.

[11] B.B. Johnsen, A.J. Kinloch, R.D. Mohammed, A.C. Taylor and S. Sprenger, (2007). Toughening mechanisms of nanoparticle-modified epoxy polymers. *Polymer*, **48 (2)**:530-541.

[12] A.J. Kinloch, R.D. Mohammed, A.C. Taylor, S. Sprenger, and D.J. Egan, (2006). The interlaminar toughness of carbon fiber reinforced plastic composites using hybrid toughened matrices, *Journal of Materials Science*, **41(15):** 5043-5046.

[13] Standard test method for tensile properties of plastics, ASTM D638, Annual book of ASTM Standards, American Society for Testing and Materials, PA, Vol. 8.02, 2003.

[14] Garg, A.C. and Mai, Y.W. (1988). Failure Mechanisms in Toughened Epoxy Resisns- A Review, *Composites Science and Technology*, **31(3):** 179-223.

[15] Standard test method for measurement of fatigue crack growth rates. ASTM E647, Annual book of ASTM standards; American Society for Testing and Materials, PA, Vol. 03.01, 1995.

[16] Zhou, Y., Pervin, F., Jeelani, S. and Mallick, P.K. (2008). Improvement in Mechanical Properties of Carbon Fabric-Epoxy Composite Using Carbon Nanofibers, *Journal of Materials Processing Technology*, **198(1-3)**: 445-453.

[17] Sauer, J.A. and Richardson, G.C. (1980). Fatigue of Polymers, *International Journal of Fracture*, **16 (6)**:499-532.

[18] J.C. Newman Jr, I.S. Raju, *Engg Fract Mech* **15**, 185 (1981).

[19] A.J Kinloch, R.D. Mohammed, A.C. Taylor, C., Eger, S. Sprenger, D Egan. *Journal of Materials Science* **40**, 5083 (2005).

[20] P.C. Paris, M.P. Gomez, W.P. Anderson, *The Trend in Engg* **13,** 9 (1961).

Table 1. The tensile properties of the epoxy polymers

Material	σ_{UTS} (MPa)	E (GPa)
Neat epoxy	73.3 ± 1.44	2.62 ± 0.05
Rubber modified epoxy	65.1 ± 1.54	2.11 ± 0.03

Table 2. The fatigue properties of the epoxy polymers

Material	Fatigue strength coefficient (FSC) σ_f' (mm/cycle)	Fatigue strength exponent (FSE) b
Neat epoxy	85.5263	-0,1205
Rubber modified epoxy	115.9044	-0.1406

Table 3. The fatigue crack growth properties of the epoxy polymers

Material	Paris' Constants		Threshold SIF
	C (mm/cycle)	m	ΔK_{th} (MPa$\sqrt{m}$)
Neat epoxy	1.2022×10^{17}	37.17	0.23
Rubber modified epoxy	1.2531×10^{-2}	7.328	0.39

Table 4. Estimated crack initiation and crack growth lives of epoxy polymers

(a) Neat epoxy

Stress σ_{max} MPa	Crack length		Crack growth life	Total fatigue life	Crack initiation life	% N_i
	a_0 (mm)	a_{cr} (mm)	N_p	N_t	$N_i=N_t-N_p$	(N_i / N_t) x 100
40.0	0.1	0.150	1	548	547	100
37.5	0.1	0.179	1	937	936	100
35.0	0.1	0.206	1	1660	1659	100
32.5	0.1	0.238	1	3071	3070	100
30.0	0.1	0.280	1	5967	5966	100
27.5	0.1	0.332	4	12284	12280	100
25.0	0.1	0.400	145	27093	26948	99

(b) Rubber-modified epoxy

40.0	0.1	0.413	545	1933	1388	72
37.5	0.1	0.468	881	3059	2178	71
35.0	0.1	0.536	1467	4997	3530	71
32.5	0.1	0.619	2534	8464	5930	70
30.0	0.1	0.721	4567	14956	10389	69
27.5	0.1	0.848	8654	27770	19116	69
25.0	0.1	1.000	17418	54699	37281	68

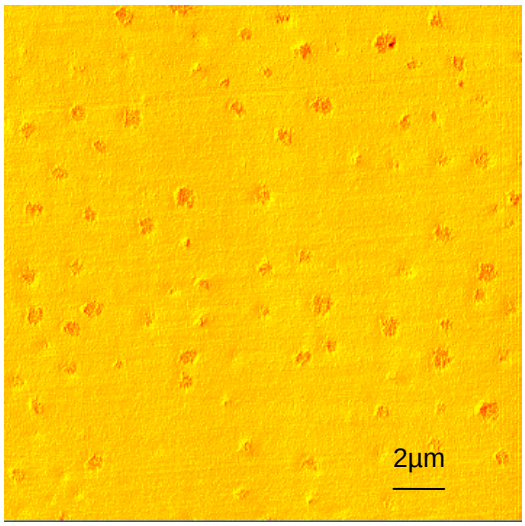
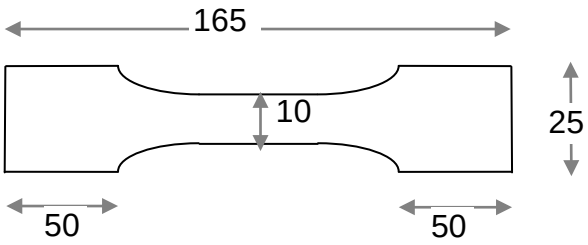
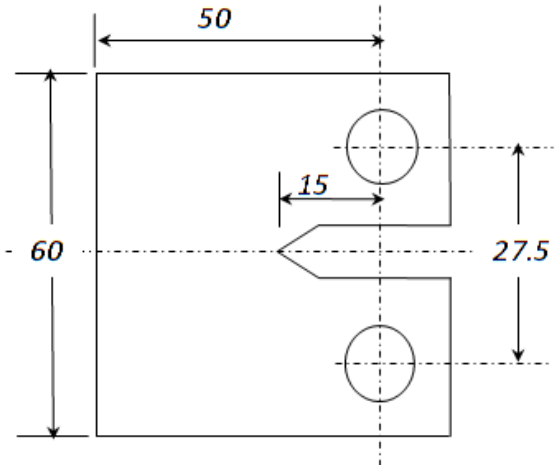


Fig. 1. The Atomic force microscopic (AFM) phase image of the rubber particle modified epoxy polymer



(a) Tensile and fatigue test specimen



(b) Fatigue crack growth test specimen

Note: All dimensions are in mm

Figure 2. Schematic diagrams showing the dimensions of the test specimens

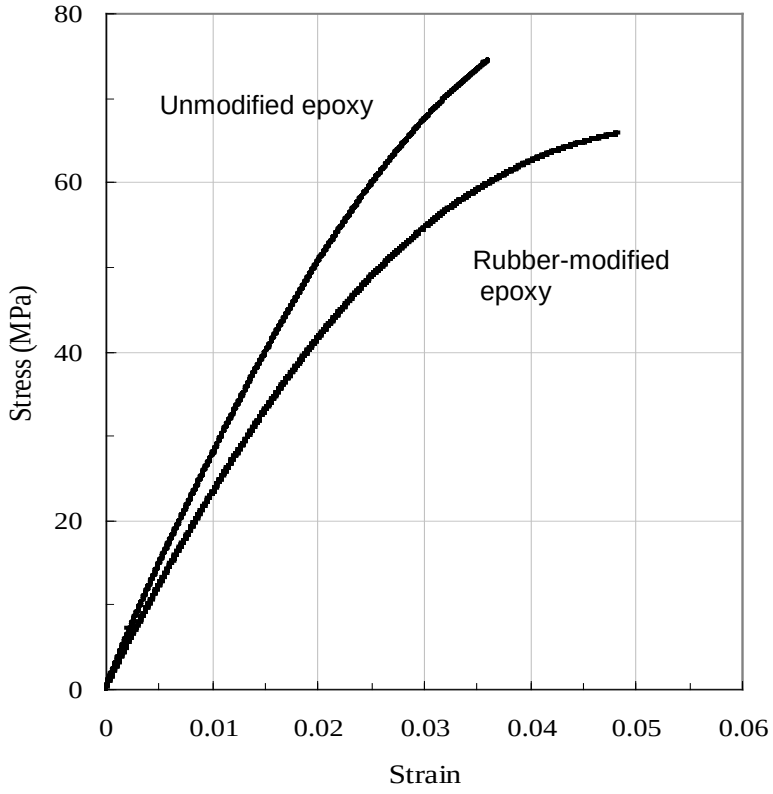


Fig. 3. The tensile behaviour of epoxy polymers

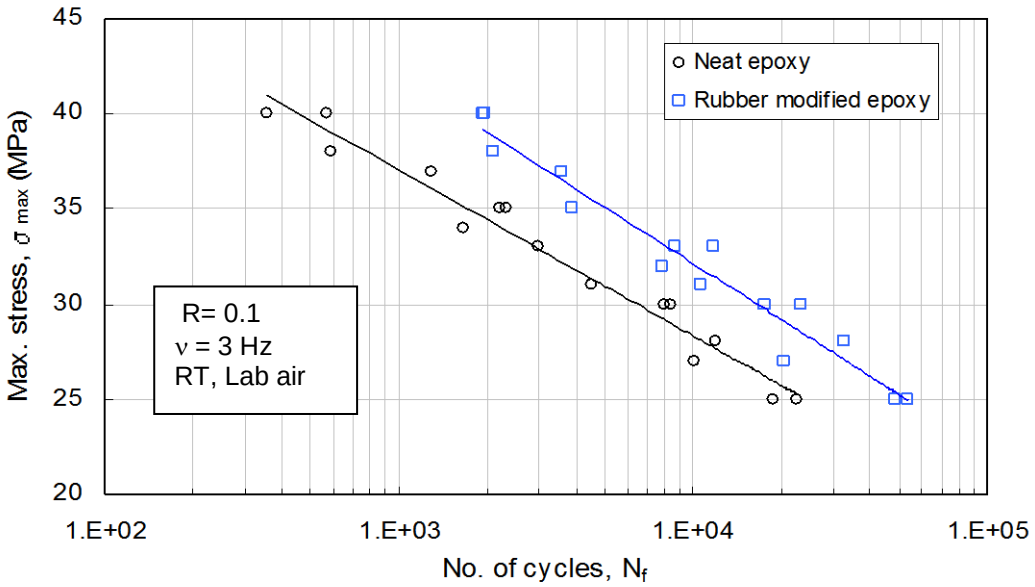
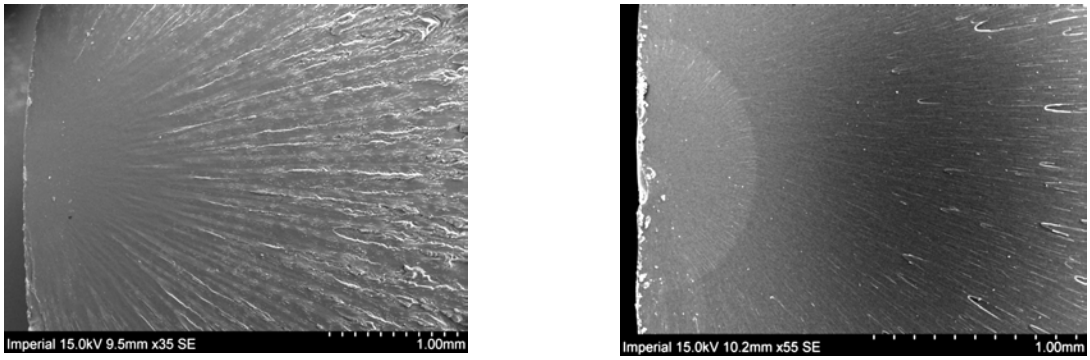


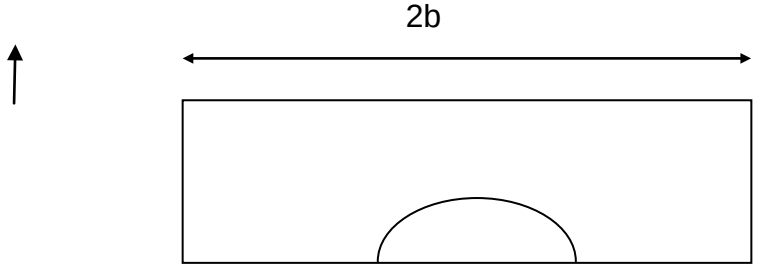
Fig. 4. The stress versus lifetime (S-N) curves of the neat and rubber modified epoxy polymers



(a) Neat epoxy (b) Rubber modified epoxy

Fig. 5. SEM micrographs showing the fatigue fracture surface of epoxies

σ_{max} = 37 MPa, R = 0.1



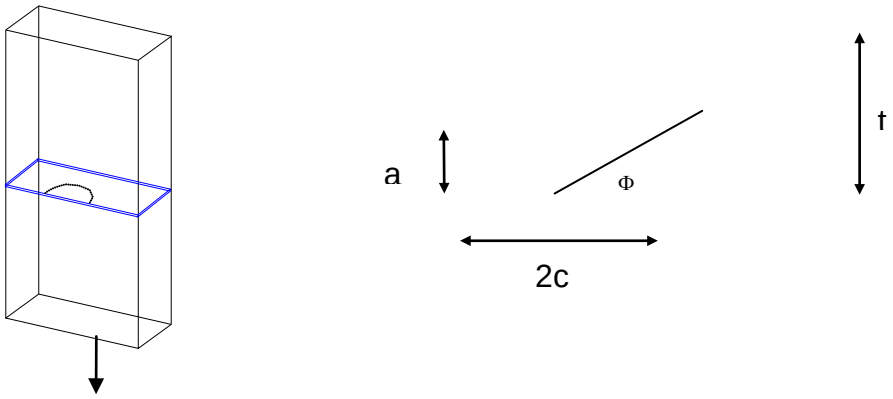


Fig. 6. A schematic of semi-elliptical surface crack in a tensile loaded, rectangular cross-sectioned specimen

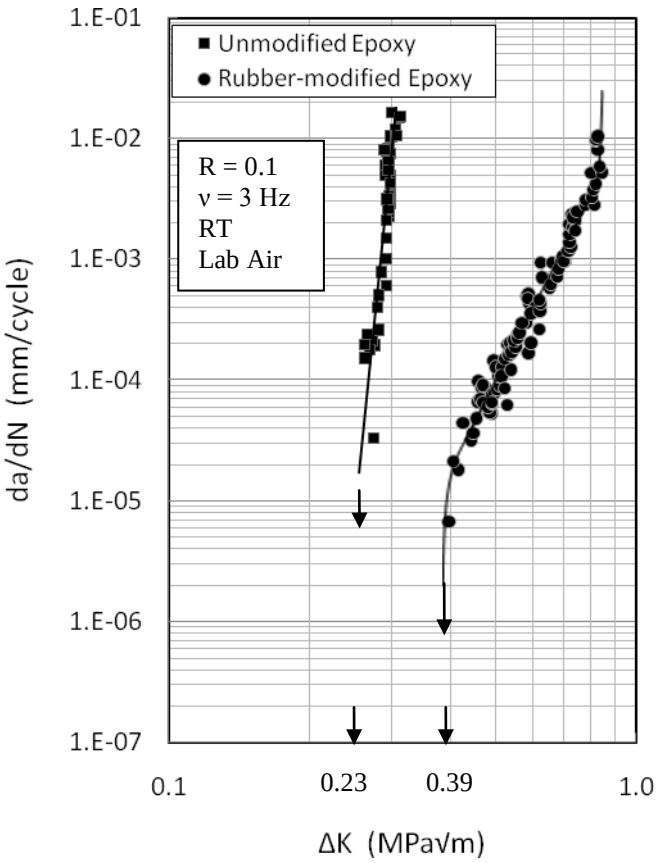


Fig. 7. The fatigue crack growth rate curves determined for epoxy polymers

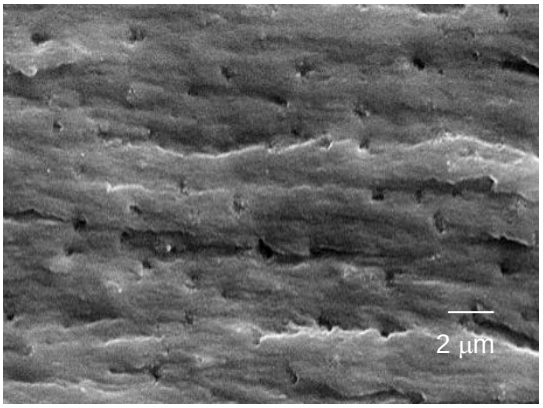


Fig. 8. SEM micrograph of the fatigue fracture surfaces of rubber-modified epoxy. R= 0.1, ~ ΔK = 0.60 MPa$\sqrt{m}$. crack growth direction is from left to right

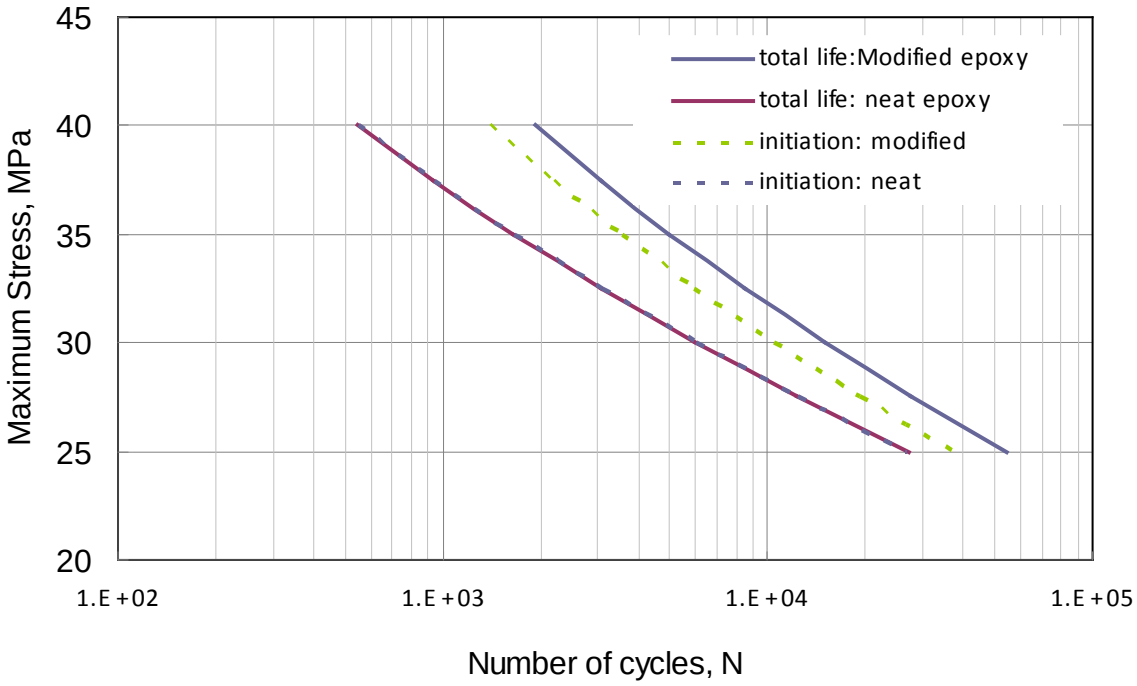


Fig. 9. Estimated crack initiation and crack propagation lives